Available online at www.sciencedirect.com
SCIENCE DIRECT
Polymer 46 (2005) 5630–5636
polymer
www.elsevier.com/locate/polymer

The crystal structure of poly(2,6-naphthalenebenzobisthiazole)

Soo-Young Park[a,*], Sang-Cheol Moon[a], Thuy D. Dang[b], N. Venkatasubramanian[c], Jar-wha Lee[d], B.L. Farmer[b]

[a]*Department of Polymer Science, Kyungpook National University, #1370 Sankyuk-dong, Buk-gu, Daegu 702-701, South Korea*
[b]*AFRL/MLBP, Wright-Patterson Air Force Base, 2941, Hobson Way, Suite 1, Dayton, OH 45433-7750, USA*
[c]*University of Dayton Research Institute, 300 College Park Drive, Dayton, OH 45469, USA*
[d]*Syscom Technology Inc., 4180, Anson Drive, Hilliard, OH 43026, USA*

Received 6 November 2004; received in revised form 21 April 2005; accepted 29 April 2005
Available online 23 May 2005

Abstract

The crystal structure of poly(2,6-naphthalenebenzobisthiazole) (Naph-2,6-PBT) was studied using X-ray and molecular modeling methods. The X-ray pattern of the annealed Naph-2,6-PBT fiber showed several Bragg reflections as well as streaks along the layer lines indicating that the registry between adjacent chains exists in the crystal with a great deal of axial disorder. Disordered structure in the crystal was fitted into the triclinic unit cell with the unit cell parameters of $a=6.78$ Å, $b=3.46$ Å, $c=14.61$ Å, $\alpha=88.0°$, $\beta=114.7°$, and $\gamma=94.8°$ with $P\bar{1}$ space group. The calculated density, 1.68 g/cm^3 was comparable with the observed density, 1.56 g/cm^3. The $\Delta c/c$ (staggering ratio) representing the registry between the adjacent chains in the *ac* plane was -0.19, which is in good agreement with the energy calculation although another local energy minimum was found at $\Delta c/c=0.31$. The disordered structure in Naph-2,6-PBT was probably due to the discrete axial shift between $\Delta c/c=0.31$ and -0.19 in the *ac* plane. The LALS refinement showed that the naphthalene group was rotated by 9 (± 3)° from the *ac* plane on the projected structure along the chain axis with a torsion angle between the naphthalene and benzobisthiazole rings of 23°.
© 2005 Elsevier Ltd. All rights reserved.

Keywords: Poly(2,6-naphthalenebenzobisthiazole); Rigid-rod polymer; Molecular modeling

1. Introduction

Rigid-rod polymers such as poly(*p*-phenylenebenzobisthiazole) (PBT) and poly(*p*-phenylenebenzobisoxazole) (PBO) have excellent thermal and thermoxidative stabilities as well as exceptional tensile strength and tensile modulus, attributable to their inherent chain stiffness and a high degree of molecular orientation, achieved by fiber-spinning from a liquid crystalline solution [1–16]. PBT and PBO fibers are thus alternatives to reinforcement aramid and carbon fibers. The crystal structures of PBO and PBT have been investigated by several research groups [17–21]. One of the prominent characteristics of PBO and PBT is the axial disorder in the crystal, which causes streaks along the layer lines in the X-ray fiber pattern. Fratini et al. [17], first reported the crystal structure of PBT in which two molecular chains pass through a metrically monoclinic unit cell with parameters of $a=11.79$ Å, $b=3.54$ Å, $c=12.51$ Å, and $\gamma=94.0°$, and the plane group of $p2$; the plane group instead of the space group can be defined as being due to the axial disorder. Fratini et al. utilized non-primitive cells in order to include longitudinal and lateral disorders because primitive cells require perfect registry of adjacent chains and close intermolecular contact occurs between neighboring molecules along the *a*-axis. Takahashi et al. [20,21] recently reported, for PBT, an oblique unit cell with parameters $a=11.60$ Å, $b=3.59$ Å, $c=12.51$ Å, and $\gamma=92.0°$ and the plane group $p2$. In the disordered structure, the molecular heights were disordered by 1/2 of the repeat distance in the *ac* plane and the molecular heights were disordered by every 1/5 of the repeat distance in the *bc* plane. The torsion angle between the benzobisthiazole and phenyl ring arises from steric interaction between the *ortho*-hydrogen on the phenyl group and the sulfur of the

* Corresponding author. Tel.: +82 53 950 5630; fax: +82 53 950 6623.
E-mail address: psy@knu.ac.kr (S.-Y. Park).

0032-3861/$ - see front matter © 2005 Elsevier Ltd. All rights reserved.
doi:10.1016/j.polymer.2005.04.070

heterocyclic ring. Fratini et al. [17] reported a torsion angle of 46° using the X-ray fiber pattern. However, a model compound for PBT showed a torsion angle of 23° [14]. Takahashi et al. [20,21], also reported a torsion angle of 20.5°, which is close to the calculated values of 27° [22,23], 20° [12], 21° [24], and 29° [25].

In the current study, the structure of Naph-2,6-PBT was delineated using X-ray and molecular modeling methods. Lower geometrical symmetry and extended planar packing of the naphthalene-2,6-diyl structural link relative to *p*-phenylene unit can affect chain conformation, packing, and crystallinity by analogy to PEN versus PET fibers [26]. The shape of the chain in the Naph-2,6-PBT is kinked compared to PBT due to the 2,6 positions at which the naphthalene group is extended. The crystal structure of Naph-2,6-PBT can be distinguished from that of PBT in terms of the axial disorder. Its crystal structure analysis would be interesting from the structural point of view as well as from the standpoint of potential enhancement of mechanical properties, especially compressive strength since the kinked structure can reduce the axial shift and increase interchain interactions.

2. Experimental

2.1. Materials

We have previously described the synthesis and general characterization of Naph-2,6-PBT [27]. Polymeric fibers were spun from the lyotropic liquid crystalline phase of the polymer in polyphosphoric acid generated during the polycondensation. Evidence for the presence of the ordered phase was obtained by the observation of optical birefringence of a sample of the dope examined by polarizing optical microscopy. Thermogravimetric analysis of the bulk polymer, isolated as a fibrous purple solid, showed that the polymer possesses exceptional thermal stability (onset of thermal degradation around 692 °C in helium and 595 °C in air). Naph-2,6-PBT fiber was fabricated by a dry-jet wet-spinning method using a custom made device. Anisotropic Naph-2,6-PBT/polyphosphoric acid (PPA) dope (10 wt% polymer) was deaerated at 100 °C and filtered through 74 μm stainless steel mesh. Napth-2,6-PBT fiber was then spun at 90 °C with a draw ratio of 40. Subsequently, the fiber was soaked in large amounts of distilled water for several days to remove any residual solvent. The air-dried fiber was then heat-treated at elevated temperatures to 550 °C in nitrogen.

2.2. X-ray analysis

Wide-angle X-ray diffraction patterns were recorded on a phosphor image plate (Molecular Dynamics©) in a Statton camera. Monochromatic Cu K_α radiation from a rotating anode X-ray generator operating at 40 KV and 240 mA was used. The sample to film distance was calibrated by Si powders. The total intensity of each Bragg reflection was measured using FIT2D software [28]. The intensity of a reflection having a maximum at 2θ (Bragg angle) and ζ (azimuthal angle) was integrated along the azimuthal direction from ζ_1 and ζ_2 at each 2θ ranging from $2\theta_1$ to $2\theta_2$ ($2\theta_1 < 2\theta < 2\theta_2$; $\zeta_1 < \zeta < \zeta_2$; $2\theta_1$, $2\theta_2$, ζ_1, and ζ_2 were chosen to include the whole area of the reflection to integrate), then the background was corrected, and finally the peak area was integrated along the 2θ angle. The structure factor was calculated after multiplicity, and the Lorenz and polarization correction [29]. The density was measured by floatation in methylene chloride and carbon tetrachloride, which are miscible non-solvents.

2.3. Molecular modeling

Molecular modeling and simulation of the X-ray patterns were performed using Cerius2® software. The conformational energy was calculated with an *ab* initio method using SPARTAN® program at the Hartree–Fock, 6-31G** level while the energy in the crystal was calculated from the discover module of Cerius2® with the consistent valence force field (CVFF) [30]. The torsion angle ϕ and rotational angle φ were defined as shown in Fig. 1(b). The rotational angle φ was defined as the angle between the *ac* plane and the naphthalene group on the projection normal to the chain axis. The conformational energies of naphthalene benzobisthiazole-2,6-diyl units were calculated at 10° increments of the torsion angle ϕ.

2.4. Refinement

The crystallographic *R* value was calculated using WinLALS software [31–33]. The bond angle and bond length were constrained with the values used in the model of PBT [17]. The parameters to be refined are the Eulerian angles which are convertible to the rotation angle φ, the torsion angle between the benzobisthiazole and naphthalene ring ϕ, the isotropic temperature factor B_{iso}, and the scale factor.

3. Results and discussion

3.1. X-ray fiber pattern

Fig. 2(a) shows the X-ray fiber pattern of Naph-2,6-PBT before annealing. Two broad strong equatorial Bragg reflections and several ordered meridional Bragg reflections were observed. This pattern is typical of an X-ray fiber pattern of an as-spun rigid-rod polymer. The *d*-spacings of the two equatorial Bragg reflections are ~6.14 and ~3.45 Å, respectively. The *d*-spacing of the second equatorial Bragg reflection (~3.45 Å) is similar to that of PBT (~3.5 Å), although that of the first equatorial Bragg

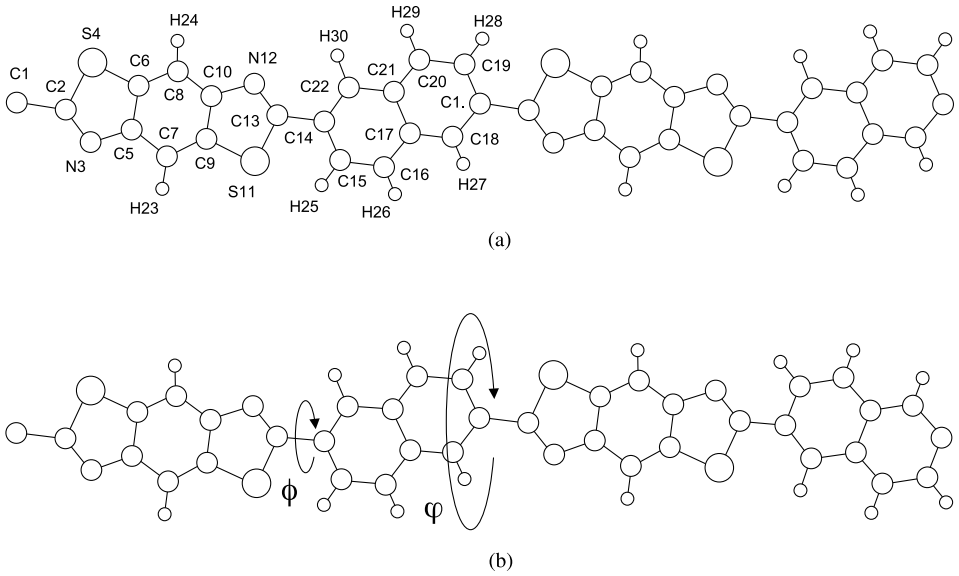

Fig. 1. The (a) *trans* and (b) *cis* conformations of Naph-2,6-PBT with the numbering of atoms: the torsion angle ϕ is S_{11}–C_{13}–C_{14}–C_{15} and rotation angle φ is 0° when the naphthalene group is parallel to the *ac* plane in the crystal and the clockwise direction is +.

reflection (~6.14 Å) has increased relative to 5.5 Å for PBT. The increase in *d*-spacing of the first equatorial Bragg reflection and the similar *d*-spacing value of the second equatorial Bragg reflection when compared to those of PBT suggests that the *d*-spacing of the side-by-side packing increases due to the large naphthalene unit although, the spacing due to the face-to-face packing is not much affected by incorporation of the naphthalene unit. The repeat distance along the chain axis, from the meridional Bragg reflection, is 14.6 Å for Naph-2,6-PBT, which is 2.1 Å longer than that of PBT; this increase is attributable to the fused aromatic ring system of the naphthalene unit. Fig. 2(b) shows the X-ray fiber pattern of Naph-2,6-PBT after annealing. The X-ray fiber pattern of the annealed Naph-2,6-PBT shows both Bragg reflections and streaks on the layer lines. The two equatorial Bragg reflections become sharper and are separated into three Bragg reflections. Only a streak on the first layer line, two distinct Bragg reflections

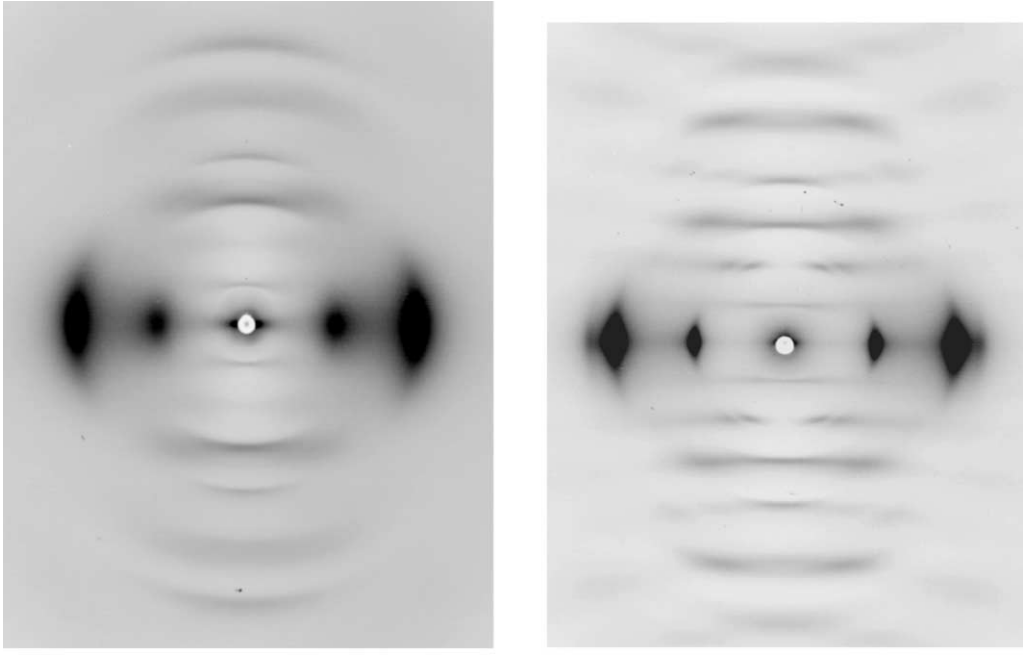

Fig. 2. X-ray fiber patterns of Naph-2,6-PBT (a) before and (b) after annealing.

on the second layer line, broad diffuse off-meridian spots connected by a rather sharp line across the meridian on the third layer line, and several broad Bragg reflections on the higher layer lines with streaks are observed. The Bragg reflections on the higher layer lines indicate that three-dimensional order is present in the crystal. However, disorder in the crystal still exists, as indicated by the streaks along the layer lines.

3.2. The crystal structure

3.2.1. Unit cell determination

The first and second strong equatorial Bragg reflections at $d=6.14$ Å and $d=3.45$ Å can be indexed as *100* and *010*, respectively. The third weak equatorial Bragg reflection in the annealed fiber pattern at $d=3.11$ Å can be indexed as *110* which gives γ^* value of 94.4° (or 180–94.4°). The two Bragg reflections on the second layer line indicate certain registry between the adjacent chains. The radius values of the cylindrical coordinates of the first and second Bragg reflection on the second layer line in the reciprocal space are 0.063 and 0.101 $Å^{-1}$, respectively. If one of the radius values of the two Bragg reflections was arbitrarily chosen as a negative value, the absolute difference between the radius values of the two Bragg reflections (0.164 $Å^{-1}$) is the same as the radius value of the *100* reflection which is the inverse of the *d*-spacing of the *100* reflection (0.163 $Å^{-1}$). This indicates that one of the two Bragg reflections can be indexed as *002* and the other as *102* (or $\bar{1}02$). If the first Bragg reflection on the second layer line was chosen as *002*, the angle between a^* and c^* (β^*) would have been 65.4°, but if the second Bragg reflection on the second layer line was chosen as *002*, β^* would have been 53.5°. Two triclinic unit cells can be obtained with unit cell parameters of $a=6.78$ Å, $b=3.46$ Å, $c=14.61$ Å, $\alpha=88.0°$, $\beta=114.7°$, and $\gamma=94.8°$ for the first set ($\beta^*=65.4°$) and $a=7.67$ Å, $b=3.47$ Å, $c=14.63$ Å, $\alpha=93.3°$, $\beta=126.6°$, and $\gamma=84.5°$ for the second set ($\beta^*=53.5°$) in which there is one chain (one monomeric unit) with the space group of $P\bar{1}$ for both unit cells. The calculated density for one monomeric unit in the unit cell is 1.68 g/cm^3 for both of the two unit cells, which is comparable to the measured density of 1.56 ($\pm$0.02) g/cm^3. The main difference between the two sets is the registry between the adjacent chains in the *ac* plane. Registry can be defined as the staggering ratio ($\Delta c/c$) where Δc is the difference in height between the adjacent chains and c is the repeat distance. The $\Delta c/c$ value is 0.19 and 0.31 for the first and second sets, respectively. The second set is more staggered than the first one due to the larger β value. The observed Bragg reflections can be indexed with both unit cells. Table 1 shows the indices of the observed Bragg reflections based on the two different unit cells. All observed Bragg reflections can be indexed with two triclinic unit cells, although some Bragg reflections (such as the *003* (index in the first set)) are too broad to determine the exact *d*-spacing. The reflections at $d=4.84$ and 4.07 Å on the third layer can be indexed only with the first and second sets, respectively, suggesting that both unit cells may be present in the real crystalline structure due to the axial disorder. The first set is more accurate when the overall *d*-spacings were compared although the *003* reflection is closer to the second set.

3.2.2. Chain conformation

Fig. 1 shows the two possible (*trans* and *cis*) conformations of Naph-2,6-PBT. The repeat distance of the *trans* conformation along the chain axis consists of the one monomeric unit, whereas that of the *cis* conformation consists of two monomeric units at the least. The fiber repeat distance is identical to the length of one repeat unit indicating that Naph-2,6-PBT adopts the *trans* conformation. There are two possible spatial dispositions of the naphthalene group in the *trans* conformation, one is for the naphthalene group being rotated toward nitrogen ($\phi=0°$) and the other is for the naphthalene group being rotated toward sulfur ($\phi=180°$). Fig. 1(a) is an example of the ring being rotated toward nitrogen. Fig. 3 shows the *ab* initio conformational energy of Naph-2,6-PBT and PBT with respect to the torsion angle, ϕ. The conformational energy of PBT is essentially the same as that reported previously [34]. The energy minima of Naph-2,6-PBT were found at $\phi=0$ and 180° with the minimum at $\phi=0°$, although the energy difference at $\phi=0$ and 180° was only 0.6 kcal/mol. In the case of PBT, the optimal torsion angle, 0°, is in poor agreement with the X-ray result found for a single crystal of 2,6-diphenylbenzobisthiazole (23.2°) [14], so the discrepancy can be attributed to crystal packing forces. However, the energy around the minimum is flat and the energy

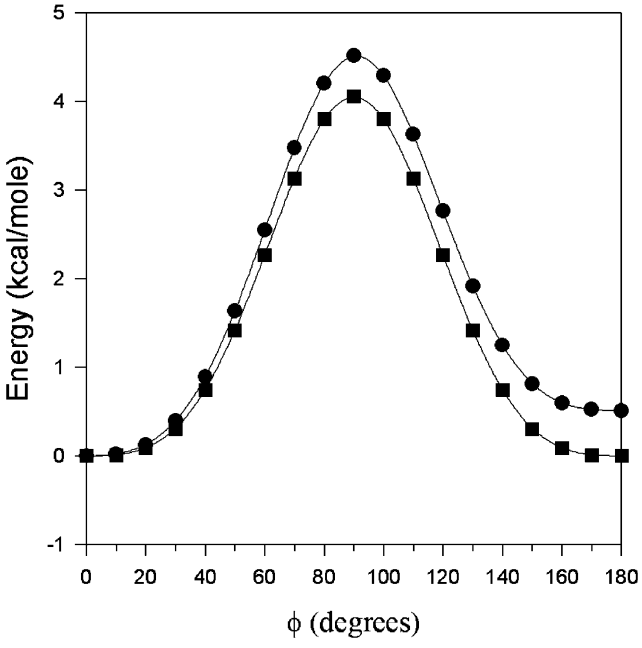

Fig. 3. The *ab* initio conformational energy of Naph-2,6-PBT (●) and PBT (■).

Table 1
The observed and calculated *d*-spacings of Naph-2,6-PBT for the first and the second sets

h	*k*	*l*	d_o (Å)	d_c (Å)
a=6.78 Å, *b*=3.46 Å, *c*=14.61 Å, α=88.0°, β=114.7°, γ=94.8°				
1	0	0	6.14	6.14
0	1	0	3.45	3.45
1	1	0	3.11	3.11
2	0	0		3.07
0	0	2	6.64	6.64
−1	0	2	5.87	5.89
			4.84[a]	
0	0	3	4.07	4.43
−1	0	4	3.64	3.62
0	0	4	3.32	3.32
−2	0	4	2.99	2.95
0	0	5	2.72	2.66
−1	1	5	2.21	2.19
1	0	5		2.14
0	0	6	2.20	2.21
a=7.67 Å, *b*=3.47 Å, *c*=14.63 Å, α=93.2°, β=126.6°, γ=84.5°				
1	0	0	6.14	6.14
0	1	0	3.45	3.45
1	1	0	3.11	3.11
2	0	0		3.07
−1	0	2	6.64	6.66
0	0	2	5.87	5.87
−1	0	3	4.84	4.86
			4.07[a]	
−1	0	4	3.64	3.61
−2	0	4	3.32	3.33
0	0	4	2.99	2.93
−1	0	5	2.72	2.82
−2	−1	5	2.21	2.28
−1	−1	5		2.22
−3	0	6	2.20	2.22

[a] The reflections at *d*=4.84 and 4.07 Å cannot be indexed with both the first and second sets.

difference at ϕ=0 and 30° is 0.31 and 0.39 kcal/mol for PBT and Naph-2,6-PBT, respectively.

3.3. The crystal structure

The streaks along the layer lines indicate axial disorders in the crystal. The projection along the *c*-axis in the crystal is not affected by the axial disorder. The equatorial *hk*0 reflections represent the projected structure along the *c*-axis. The equatorial *hk*0 reflections of the crystal are affected by the torsion and rotation angles because there is one chain in the unit cell. The final parameters are obtained by the constrained LALS method. The refinement converged at *R*=1.37%. The structure factors for the three reflections are (62.6, 160.8, 75.8) and (61.6, 160.7, 75.7) for the observed and calculated ones, respectively. Regarding the small B_{iso}, 0.12 may be attributed to the rigidity of the molecules [35]. Two parameters, torsional angle ϕ and rotational angle φ determine chain packing because the unit cell contains one monomeric unit (a single polymer chain). The rotation angle is −9 (±3)° which means that the naphthalene ring is nearly parallel to the *ac* plane. The torsion angle, ϕ=∼23°, is the same as that of PBT.

Fig. 4 shows the calculated energy of the crystal with respect to the staggering ratio ($\Delta c/c$) in the *ac* plane while keeping the same *ab* projection of the crystal structure. The unit cell was calculated by changing β* and keeping the other reciprocal lattice parameters constant. The calculated unit cell has the same *ab* projection in the real space and the staggering ratio can be controlled by β*. The minimum energy was found at $\Delta c/c=-0.20$. The value of $\Delta c/c=-0.20$ was close to that of the first set of the two possible unit cells ($\Delta c/c=-0.19$). The staggering at $\Delta c/c=0.31$ for the second set constitutes another local minimum. The energy calculation suggests that the first set is more plausible than the second one. However, a lot of possibilities exist for the axial disorder to occur between these two staggering ratios.

Fig. 5 shows projections of the models of Naph-2,6-PBT for the first set of the unit cells. The fractional coordinates are given in Table 2. In the projection along *c*-axis (Fig. 5(c)), the chains are packed closely and the naphthalene rings are rotated by −9(±3)° from the *ac* plane. In the *ac* projection (Fig. 5(a)), the kinked chains of Naph-2,6-PBT are staggered side-by-side by 0.19*c*. The 0.19*c* staggering between the adjacent chains provides optimum packing in crystal without any steric interaction.

4. Conclusions

We found that in general, the X-ray fiber pattern of Naph-2,6-PBT is similar to that of PBT in terms of reflections as well as the streaks along the layer lines. This X-ray fiber pattern suggests that the registry between adjacent chains exists in the crystal with significant axial disorder. The *d*-spacings of the two equatorial Bragg reflections are ∼6.14 and ∼3.45 Å. The *d*-spacing of the second equatorial Bragg reflection (∼3.45 Å) is similar to that of PBT (∼3.5 Å), although the first equatorial Bragg reflection (∼6.14 Å) is increased compared to that of PBT (5.5 Å). The increase in *d*-spacing of the first equatorial Bragg reflection and the similar *d*-spacing of the second equatorial Bragg reflection relative to those of PBT suggest that the spacing of the side-by-side packing increases due to the large naphthalene unit, although the spacing due to the face-to-face chain packing was not much affected by the incorporation of the naphthalene unit. The fiber repeat distance was 14.6 Å which is larger compared to that of PBT (12.5 Å). Presumably, the longer repeat length is due to the fused aromatic ring system of the naphthalene unit. The main difference between the X-ray fiber patterns of Naph-2,6-PBT and PBT was due to the Bragg reflections on the second layer lines. The Bragg reflection of PBT on the second layer line was separated into two Bragg reflections for Naph-2,6-PBT. The extent of staggering between the adjacent chains could be determined from the Bragg

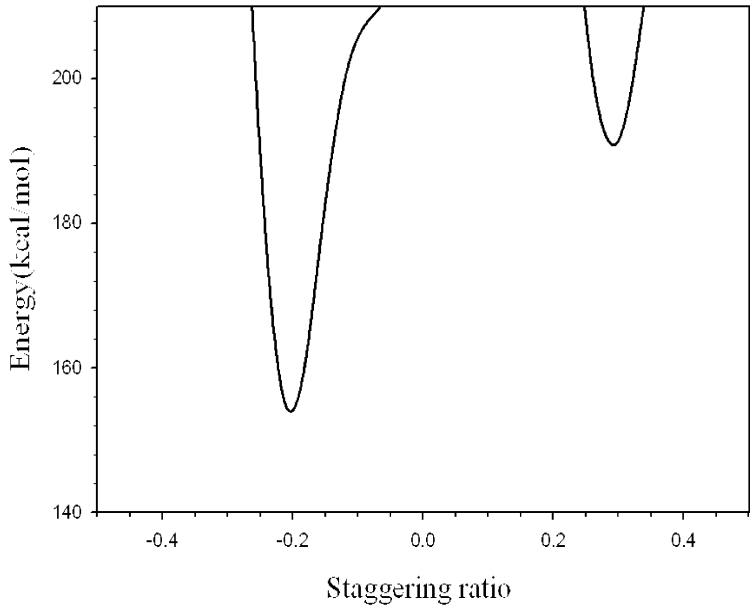

Fig. 4. The energy of the crystal versus the staggering ratio ($\Delta c/c$) in the *ac* plane keeping the same *ab* projection of the crystal structure.

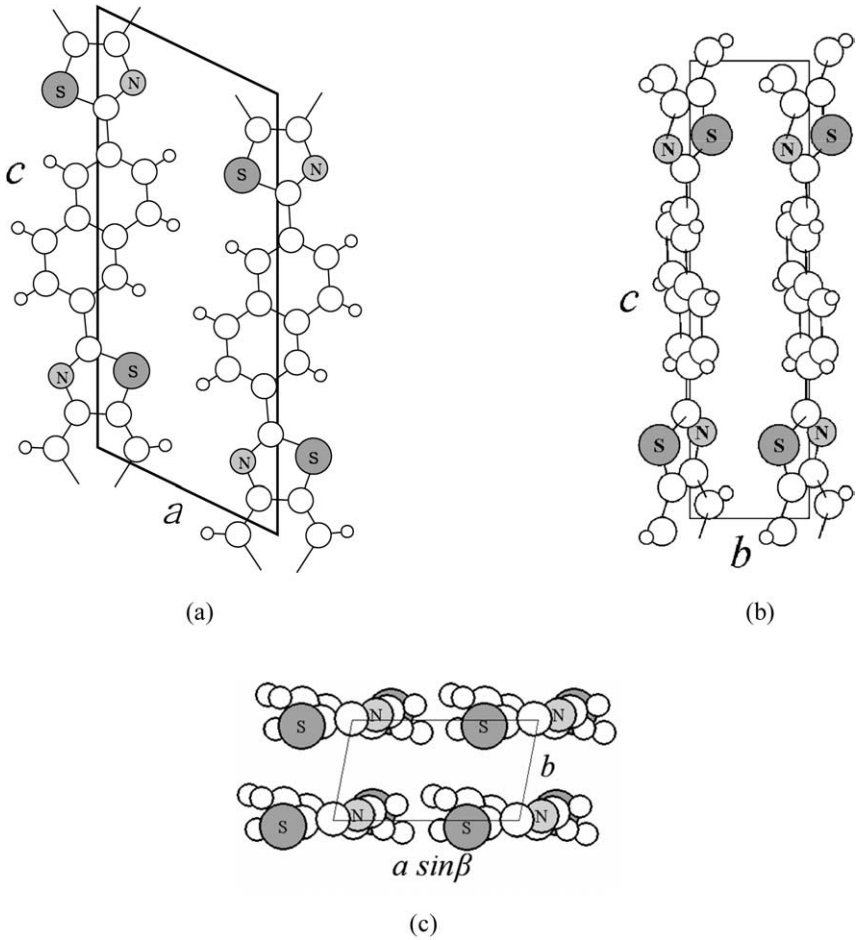

Fig. 5. The projections of the models of Naph-2,6-PBT: (a) the *ac* projection; (b) the *bc* projection; (c) the projection down *c* edge; S, sulfur; N, nitrogen.

Table 2
Fractional coordinates

Atom	X	Y	Z
S4	0.2386	−0.1267	0.1839
C2	−0.0179	−0.0235	0.2317
N3	−0.1730	0.0507	0.1745
C5	−0.0982	0.0307	0.0852
C6	0.1264	−0.0641	0.0758
C8	0.2264	−0.0957	−0.0082
C10	0.0990	−0.0307	−0.0852
N12	0.1730	−0.0504	−0.1745
C13	0.0179	0.0235	−0.2317
S11	−0.2386	0.1267	−0.1839
C9	−0.1264	0.0643	−0.0758
C7	−0.2259	0.0957	0.0083
H23	−0.3757	0.1588	0.0150
C14	0.0459	0.0249	−0.3316
C15	0.2555	0.0838	−0.3688
C16	0.2855	0.0864	−0.4621
C17	0.1059	0.0299	−0.5221
C21	−0.1055	−0.0296	−0.4847
C20	−0.2852	−0.0864	−0.5447
C19	−0.2554	−0.0838	−0.6380
C18	0.1318	0.0307	−0.6189
H27	0.2717	0.0701	−0.6450
H28	−0.3796	−0.1232	−0.6775
H29	−0.4265	−0.1261	−0.5201
C22	−0.1316	−0.0307	−0.3879
H30	−0.2720	−0.0701	−0.3621
H26	0.4269	0.1261	−0.4868
H25	0.3765	0.1220	−0.3293
H24	0.3764	−0.1603	−0.0042
C1	−0.0458	−0.0249	−0.6744
C1	−0.0458	−0.0249	0.3316

reflections on the second layer line. One of the two Bragg reflections can be indexed as *002* and the other as *102* (or $\bar{1}02$). From indexing the two Bragg reflections, two triclinic unit cells were proposed with unit cell parameters of $a=6.78$ Å, $b=3.46$ Å, $c=14.61$ Å, $\alpha=88.0°$, $\beta=114.7°$, and $\gamma=94.8°$ for the first set and $a=7.67$ Å, $b=3.47$ Å, $c=14.61$ Å, $\alpha=86.7°$, $\beta=126.6°$, and $\gamma=95.5°$ for the second set in which there is one chain (one monomeric unit) with the $P\bar{1}$ space group. The better agreement in *d*-spacing was found in the first set. The difference between the two sets is the registry between the adjacent chains in the *ac* plane; the $\Delta c/c$s (staggering ratio) are -0.19 and 0.31 for the first and second sets, respectively, and the energy minimum was found at $\Delta c/c=-0.19$ and the local energy minimum was found at $\Delta c/c=0.31$. The axial disorder might have originated from the random axial shift between the adjacent chains by -0.19 or 0.31 of the repeat distance in the *ac* plane. LALS refinement showed that the naphthalene group was rotated by -9 $(\pm 3)°$ from the *ac* plane on the projected *ab* plane with a torsion angle between the naphthalene and the heterocyclic ring of 23°, which is the same as that of PBT.

Acknowledgements

This work was supported by grant No. R08-2003-000-10338-0(2004) from the Basic Research Program of the Korea Science and Engineering Foundation and Brain Korea 21 program. We appreciate Prof Kenji Okuyama (Tokyo University of Agriculture and Technology) for the fruitful discussions and supplying the winLALS program.

References

[1] Ulrich DR. Polymer 1987;28:533.
[2] Roche EJ, Takahashi T, Thomas EL. ACS Symp Ser 1980;141:303.
[3] Odell JA, Keller A, Atkins EDT, Miles MJ. J Mater Sci 1981;116:3309.
[4] Adams WW, Eby RK. MRS Bull 1987;12:22.
[5] Allen SR, Filippov AG, Farris RJ, Thomas EL, Wong CP, Berry GC, et al. Macromolecules 1981;14(4):1135.
[6] Wolfe JF, Arnold FE. Macromolecules 1981;14:909.
[7] Wolfe JF, Loo BH, Arnold FE. Macromolecules 1981;14(4):915.
[8] Choe EW, Kim SN. Macromolecules 1981;14:920.
[9] Cotts DB, Berry GC. Macromolecules 1981;14:930.
[10] Welsh WJ, Bhaumik D, Mark JE. Macromolecules 1981;14:947.
[11] Welsh WJ, Bhaumik D, Jaffee HH, Mark JE. Polym Eng Sci 1984;24:218.
[12] Welsh WJ, Mark JE. J Mater Sci 1983;18:1119.
[13] Bhaumik D, Welsh WJ, Jaffee HH, Mark JE. Macromolecules 1981;14(4):951.
[14] Wellman MW, Adams WW, Wolff RA, Dudis DS, Wiff DR, Fratini AV. Macromolecules 1981;14:935.
[15] Chu SG, Venkatraman S, Berry GC, Einaga Y. Marcromolecules 1981;14(4):939.
[16] Wierschke SG. Master Thesis. Ohio: Wright State University; 1988.
[17] Fratini AV, Lenhert PG, Resch TJ, Adams WW. Mater Res Soc Symp Proc 1989;134:431.
[18] Martin DC, Thomas EL. Macromolecules 1991;24:2450.
[19] Tashiro K, Yoshino J, Kitagawa T, Murase H, Yabuki K. Macromolecules 1998;31:5430.
[20] Takahashi Y. Macromolecules 1999;32:4010.
[21] Takahashi Y. Macromolecules 2001;34:2012.
[22] Welsh WJ, Mark JE, Yang Y, Das GP. Mater Res Soc Symp Proc 1989;134:621.
[23] Yang Y, Welsh WJ. Macromolecules 1990;23:2410.
[24] Welsh WJ, Yang Y. Comp Polym Sci 1991;1:139.
[25] Farmer BL, Wierschke SG, Adams WW. Polymer 1990;31:1631.
[26] Tonelli AE. Polymer 2002;43:637.
[27] Dang TD, Venkatasubramanian N, Talicska A, Park SY, Arnold FE. Polym Prepr (Am Chem Soc) 2002;43(1):660.
[28] www.esrf.fr/computing/scientific/FIT2D/
[29] Okuyama K, Noguchi K, Miyazawa T, Yui T, Ogawa K. Macromolecules 1997;30:5849.
[30] www.accelrys.com/doc/life/cerius46/
[31] Arnott S, Wonacott S. Polymer 1966;7:157.
[32] Smith PJC, Arnott S. Acta Crystallogr Sect A 1978;34:3.
[33] Okada K, Noguchi K, Okuyama K, Arnott S. Comput Biol Chem 2003;27:265.
[34] Trohalaki S, Dudis DS. Polymer 1995;36(5):911.
[35] Takahashi Y, Sul H. J Polym Sci, B: Polym Phys 2000;38:376.